

Mechanisms of extracellular S⁰ globule production and degradation in *Chlorobaculum tepidum* via dynamic cell–globule interactions

C. L. Marnocha,^{1,2} A. T. Levy,^{2,3} D. H. Powell,² T. E. Hanson^{2,4,5} and C. S. Chan^{1,2,4}

Correspondence
C. S. Chan
cschan@udel.edu

¹Department of Geological Sciences, University of Delaware, Newark, DE 19716, USA

²Delaware Biotechnology Institute, University of Delaware, Newark, DE 19711, USA

³Department of Chemical and Biomolecular Engineering, University of Delaware, Newark, DE 19716, USA

⁴School of Marine Science and Policy, University of Delaware, Newark, DE 19716, USA

⁵Department of Biological Sciences, University of Delaware, Newark, DE 19716, USA

The *Chlorobiales* are anoxygenic phototrophs that produce solid, extracellular elemental sulfur globules as an intermediate step in the oxidation of sulfide to sulfate. These organisms must export sulfur while preventing cell encrustation during S⁰ globule formation; during globule degradation they must find and mobilize the sulfur for intracellular oxidation to sulfate. To understand how the *Chlorobiales* address these challenges, we characterized the spatial relationships and physical dynamics of *Chlorobaculum tepidum* cells and S⁰ globules by light and electron microscopy. *Cba. tepidum* commonly formed globules at a distance from cells. Soluble polysulfides detected during globule production may allow for remote nucleation of globules. Polysulfides were also detected during globule degradation, probably produced as an intermediate of sulfur oxidation by attached cells. Polysulfides could feed unattached cells, which made up over 80% of the population and had comparable growth rates to attached cells. Given that S⁰ is formed remotely from cells, there is a question as to how cells are able to move toward S⁰ in order to attach. Time-lapse microscopy shows that *Cba. tepidum* is in fact capable of twitching motility, a finding supported by the presence of genes encoding type IV pili. Our results show how *Cba. tepidum* is able to avoid mineral encrustation and benefit from globule degradation even when not attached. In the environment, *Cba. tepidum* may also benefit from soluble sulfur species produced by other sulfur-oxidizing or sulfur-reducing bacteria as these organisms interact with its biogenic S⁰ globules.

Received 26 October 2015
Accepted 25 April 2016

INTRODUCTION

Solid elemental sulfur (S⁰) is an intermediate in the microbial oxidation of sulfide or thiosulfate to sulfate. Some sulfur-oxidizing bacteria (SOB) are able to both produce and degrade globular S⁰, often as a required intermediate step in the complete oxidation of sulfide to sulfate. The SOB are physiologically and phylogenetically diverse (Friedrich *et al.*, 2001; Gregersen *et al.*, 2011), and as a result, so are the ways and means of sulfur globule

production and degradation. One of the most significant variations in SOB is where sulfur globules are deposited: intracellularly or extracellularly (Dahl & Prange, 2006). The green sulfur bacterium (GSB) *Chlorobaculum tepidum*, the model organism of the *Chlorobiales*, produces and degrades extracellular S⁰ globules (Chan *et al.*, 2008c; Overmann & Garcia-Pichel, 2013). Because *Cba. tepidum* and other *Chlorobiales* deposit S⁰ globules extracellularly, several obstacles must be overcome in both production and degradation stages of globule metabolism. Despite the fundamental nature of these obstacles, little is understood about the spatial relationships and interactions between *Cba. tepidum* and S⁰ globules.

In the production of globules, sulfide is oxidized in the periplasm of these Gram-negative bacteria to S⁰ and must

Abbreviations: cryoSEM, cryo-scanning electron microscopy; GSB, green sulfur bacteria; SOB, sulfur-oxidizing bacterium.

Four supplementary videos and four supplementary figures are available with the online Supplementary Material.

be exported outside of the cell through some mechanism (Gregersen *et al.*, 2011; Hanson *et al.*, 2015). This mechanism should also prevent the encrustation of cells by the mineral. For iron-oxidizing microbes, strategies evolved to avoid encrustation include the formation of extracellular structures (Chan *et al.*, 2011), cell surface tuning (Saini & Chan, 2013) and changing cellular microenvironments (Hegler *et al.*, 2010). These strategies work to direct mineral formation away from the cell surface, allowing cells to avoid complete entombment. In contrast to Fe-oxidizing microbes, strategies used by SOB to avoid encrustation are currently unknown.

Once sulfide has been depleted, *Cba. tepidum* will begin to oxidize S^0 . How S^0 in extracellular globules is accessed by cells is not well understood. However, two general mechanisms have been proposed: direct contact and at-a-distance degradation (Chan *et al.*, 2008a; Lloyd, 2003). Direct contact requires physical contact between the surface of the cell or cellular appendages (e.g. pili). This is analogous to the metal-reducing mechanisms of *Shewanella putrefaciens* MR-1, where outer membrane cytochromes are implicated in the direct-contact reduction of Mn(IV) and Fe(III) (Beliaev & Saffarini, 1998; Myers & Myers, 1992; Shi *et al.*, 2009). At-a-distance mechanisms require the excretion of reducing substances or electron carriers that can act on solid substrates some distance from the cell. In the Fe-reducer *Geobacter sulfurreducens*, dissolved cytochromes can shuttle electrons to less accessible electron acceptors such as Fe(III) oxides (Lloyd *et al.*, 1999). In other Fe-reducing bacteria, humic substances, flavins and anthraquinone-2,6-disulfonate can also serve as electron shuttles (Fuller *et al.*, 2014; Gralnick & Newman, 2007; Lovley *et al.*, 1996; Marsili *et al.*, 2008).

Studies of other SOB have suggested a direct contact mechanism for insoluble sulfur degradation. *Allochromatium vinosum*, a purple sulfur bacterium, requires attachment to use exogenously provided solid sulfur substrates (Franz *et al.*, 2007). In addition, Mangold *et al.* (2011) suggest that unattached cells of *Acidithiobacillus caldus*, a chemotrophic sulfur oxidizer, are starved compared with cells attached to biologically produced S^0 particles. Within the GSB, *Chlorobaculum parvum* has also been shown to require contact with elemental sulfur in order to utilize it (Donà, 2011).

Recently, we reported the ability of *Cba. tepidum* to grow on biogenic S^0 globules as the sole photosynthetic electron donor and demonstrated that cellular attachment was required for growth on S^0 (Hanson *et al.*, 2015). Building on those methods and results, here we use time-lapse light microscopy and electron microscopy to characterize the spatial relationships and attachment dynamics of *Cba. tepidum* cells and S^0 globules during both globule production and degradation. We show that attachment of cells and sulfur globules is dynamic and largely transient. These observations are in contrast to reports of mostly attached globules that were referred to as 'functionally intracellular'

in some other *Chlorobiales* (Then & Trüper, 1984; Trüper & Genovese, 1968; van Gemerden, 1986). We propose a model of sulfur globule production and degradation in *Cba. tepidum* that includes a combination of both direct contact and remote mechanisms to explain our results. This model can account for the growth of attached and unattached cells, and the production and degradation of both attached and unattached sulfur globules.

METHODS

***Cba. tepidum* cultures.** *Cba. tepidum* strain WT2321 was used in all cultures and grown in either Pf-7 medium (Chan *et al.*, 2008c) or sulfur-free Pf-7 medium where thiosulfate and sulfide were initially omitted and individual tubes were amended with 2.5 mM sulfide prior to inoculation. All culture media were buffered to pH 6.9–7.0 with 10 mM Bis-Tris-propane. Standard growth conditions were 47 °C and 20 $\mu\text{mol photons m}^{-2}\text{s}^{-1}$ from GE incandescent bulbs, as measured with a light meter equipped with a quantum PAR sensor (LI-COR). Primary cultures from cryo-stocks were grown under these conditions for 40–48 h, and then used to inoculate secondary cultures used in time-lapse imaging or electron microscopy.

Time-lapse light microscopy. Live cultures of *Cba. tepidum* were loaded into borosilicate rectangular capillary tubes (VetroCom). Capillaries were then sealed at both ends with epoxy and mounted on a glass slide for viewing on a Zeiss AxioImager Z1 light microscope. The microscope stage was fitted with a heated glass plate (Tokai Hit) set to 47 °C. An objective lens heater (Tokai Hit) set to 37 °C was used on a $\times 40$ EC Plan NeoFluar lens with a numerical aperture of 0.75 and resolution of 0.45 μm (Zeiss). A shield was placed around the microscope to minimize thermal drift. Light was provided at approximately 20 $\mu\text{mol photons m}^{-2}\text{s}^{-1}$ from GE incandescent bulbs over the course of the time-lapse experiments. Light flux was measured as described above. All time-lapse imaging was done under phase contrast at $\times 400$ total magnification with a Zeiss AxioCam Mrm camera, and AxioVision software was used to capture images every minute for hour-long experiments.

The effect of light on cell motion was tested by incubations without a light source except the brief illumination used only during imaging (76 ms per image). The effect of cell viability on motion was tested by fixing cells with 2.5% glutaraldehyde prior to capillary loading, with illumination as described above.

Image analysis. Time-lapse microscopy images were analysed in Fiji (Schindelin *et al.*, 2012) and Volocity software (PerkinElmer). Cells and sulfur were separated via image thresholding for counts and interaction analyses. Automated counts were compared against manual counts to confirm reliability of the thresholding method for analysis. Fiji was also used to construct time-lapse montages. Brightness and contrast of micrographs were adjusted for clarity. The 2D Particle Distribution plugin from the BioVoxxel suite was used to determine the spatial relationships between sulfur globules (Brocher, 2015). This plugin determines if particles distributed on a 2D plane are likely to be randomly distributed, self-avoiding or clustered. Nearest neighbour distances were calculated for each particle and compared against the theoretical nearest neighbour distance. The median nearest neighbour distance was statistically compared with the theoretical one using an *F*-test and then evaluated with a Welch's *t*-test. The plugin uses statistical hypothesis tests to determine if the estimated interaction is significant. Cell movement was tracked in time-lapse movies using the Manual Tracking plugin in Fiji. Movie images were aligned and individual cells were tracked every 10 min throughout the course of the time-lapse.

Cryo-scanning electron microscopy and transmission electron microscopy. Samples were prepared for cryo-scanning electron microscopy (cryoSEM) either on filters or on ACLAR (Honeywell/Allied Signal), a fluoropolymer film. Filtered samples were prepared by carefully pipetting culture onto 0.2 µm pore size polycarbonate filters (Millipore) and gently washed with deionized water. For ACLAR samples, strips of ACLAR were autoclaved and added to tubes, which were then filled with S-free Pf7 medium in an anaerobic chamber. Tubes were then stoppered and sealed, followed by headspace exchange and pressurization to 10 p.s.i. (~69 kPa) with 5% CO₂ + 95% N₂ gas passed through heated copper. At least 24 h prior to inoculation, ACLAR tubes were amended with 2.5 mM sulfide. ACLAR tubes were then inoculated, with care taken to inject inoculum over the ACLAR strip. Tubes were incubated as described above, but secured horizontally in the water bath. Following incubation, the ACLAR strip was removed and cut to size for imaging. Samples were mounted onto specimen holders with Tissue Freezing Medium (Electron Microscopy Sciences).

Samples were plunged into liquid nitrogen slush and transferred under vacuum to the Gatan Alto 2500 cryo chamber at a temperature of -120 °C. Samples were then sublimated for 10 min at -90 °C followed by cooling to -120 °C. A thin layer of gold-palladium was sputtered onto the samples. The samples were then transferred into a Hitachi S-4700 field-emission scanning electron microscope for imaging.

For transmission electron microscopy imaging, formvar/carbon-coated 400 mesh copper grids were glow discharged with a Pelco easiGlow system to render the surface hydrophilic. The grid was then floated on a drop of sample for several seconds, washed on four drops of filtered deionized water and then negatively stained with 2% aqueous uranyl acetate. Samples were imaged on a Zeiss Libra 120 transmission electron microscope equipped with a Gatan Ultrascan 1000 CCD camera.

Reduced sulfur compound analysis by HPLC. Cultures were grown in sulfur-free PF-7 medium with either 2.1 mM sulfide or 9.1 mM biogenic S⁰ [purified as described by Hanson *et al.* (2015)] as the sole electron donor. Samples for analysis were taken during the exponential growth phase before the electron donor was exhausted. Cells and globules were removed by centrifugation (16 400 g, 2 min) and a sample of the supernatant was immediately used for bismine derivatization following previously described methods (Chan *et al.*, 2008c). This method can

quantify thiosulfate, sulfite and sulfide at concentrations >1 µM. Polysulfides are detected by this method, but cannot be accurately quantified (Rethmeier *et al.*, 1997). The polysulfide standard was prepared by adding an anoxic sulfide solution to solid S₈ (2:1 molar ratio of S₈/sulfide) in a sealed tube under an atmosphere of 5% CO₂ + 95% N₂.

RESULTS

Motility in *Cba. tepidum* results in dynamic interactions with S⁰ globules

We used time-lapse light microscopy of live *Cba. tepidum* cultures to determine how the spatial relationships of *Cba. tepidum* cells and S⁰ globules changed over time. The attachment of cells to S⁰ globules was dynamic, with attached cells frequently detaching and reattaching, sometimes to multiple globules. As a result, some globules within the population were observed to be free from cells for over six consecutive hours during both production and degradation stages. Multiple cells would also attach to a single globule, with some remaining attached over time, and others attaching to the globule for only several minutes. Considering the consistent observations of attachment and detachment of cells to S⁰ globules and movement between different globules, we questioned how a microbe that is considered non-motile could cover distances of tens of micrometres. Cells tracked in live, illuminated cultures moved an average total distance of 26 µm and an average net distance of 7 µm (Fig. 1a, Video S1, available in the online Supplementary Material) over 6.5 h. To rule out Brownian motion as the primary cause of cellular motion, we performed equivalent time-lapse experiments on live cells in the dark, as well as glutaraldehyde-killed cells in light, at 47 °C; in both cases, cells showed no net movement (Fig. 1b, c; Videos S2 and S3). These results clearly demonstrate that *Cba. tepidum* is motile.

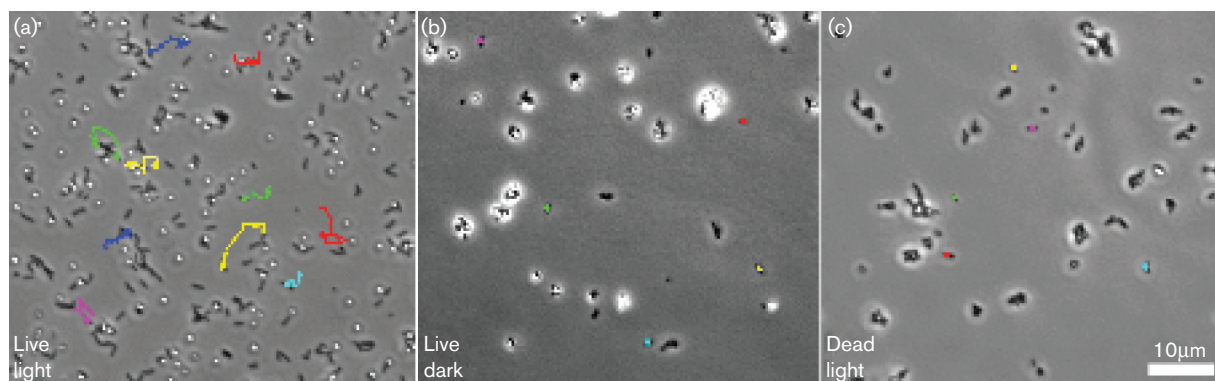


Fig. 1. Cell movement paths for (a) an illuminated, live culture (Video S1); (b) a live culture in the dark (Video S2); and (c) an illuminated, glutaraldehyde-killed culture (Video S3). Cell paths were tracked for the duration of the time-lapse (6 h 40 min, 10 h and 10 h, respectively), and overlaid on the final frame of the time-lapse (line represents the path, dot represents final position). Nearly all cells in the illuminated, live culture moved; the few cells that did not appear to move were attached to globules, which remained in fixed positions. Cell paths in killed and dark cultures never exceeded the diameter of the final position marker ($d=1.6\ \mu\text{m}$). All cultures were heated at 47 °C during imaging.

To find a genetic basis for the observed cellular movement, the *Cba. tepidum* genome was examined for the presence of genes that might confer motility. A cluster of 18 genes (CT0425–CT0442) encoding homologues of type IV pilin subunits, pilus assembly proteins and hypothetical proteins is present in the *Cba. tepidum* genome. Type IV pili are responsible for twitching motility and tight surface adherence (Burrows, 2012; Kachlany *et al.*, 2001). We observed the presence of structures with similar dimensions to type IV pili in *Cba. tepidum* cells using TEM imaging (Fig. 2). Twitching motility is driven by ATPases that polymerize and depolymerize pilin subunits. Polymerization extends the pilus from the cell, allowing it to attach to a surface, while depolymerization pulls the cell along the attached pilus (Maier & Wong, 2015). This cluster contains two candidate ATPases involved in protein secretion (CT0433 and CT0434) along with orthologues of subunits required for type IV pilus assembly (CT0435 and CT0436). The annotation for gene CT0437 notes that it contains an authentic frameshift mutation. We sequenced CT0437 in our laboratory strain of *Cba. tepidum*; the sequence matched the published genome perfectly (data not shown). The amino acid sequence derived from CT0437 is homologous to the type IV leader peptidase superfamily (peptidase A24, pfam01478), which is involved in the maturation of pilin subunits in diverse organisms (Berry & Pelicic, 2015). Because the frameshift mutation leaves the peptidase gene product largely intact, we expect the gene cluster to be sufficient for the motility we observe in *Cba. tepidum*.

S⁰ globule nucleation and growth can occur at a distance from cells

We tracked the formation of globules in the production stage using time-lapse phase contrast light microscopy (Fig. 3). S⁰ globules first became visible within the first 30 min of illuminated incubation, upon reaching approximately 0.5 µm in diameter, just over the 0.45 µm resolution of the lens used for imaging, and appeared phase-dark at this size. No new globules became visible after this point and the existing globules increased in apparent diameter. S⁰ globules transitioned to phase-bright once they exceeded 1 µm in diameter.

Globules became visible and grew in size at a distance from cells, in some cases without any contact by cells throughout the entire production stage (Fig. 3, Video S1). Over 50% of globules received only transient cell contact throughout the lifetime of the globule. The largest distance observed between a newly formed globule and a cell was approximately 8 µm, with typical distances closer to 4 µm (Fig. S1). In rare cases, globules became visible and grew with cells attached for much of the production stage. Growth rates were similar for globules always in cell contact versus those never in cell contact (Fig. S2) and globule growth rates did not depend on the number of cells in close proximity (Fig. S3). However, because total globule growth was similar to

the imaging resolution (0.45 µm), no statistical evaluation could be made.

Cells outnumbered S⁰ globules for the duration of the time-lapse experiment. The ratio of cells to globules in the production stage was 1.5–2.5, increasing in that range over time as cells divided, but no new globules formed. The spatial distribution of globules in the time-lapse field of view was non-random and clustered ($P < 0.001$) based on the median nearest neighbour distance compared with a theoretical random distribution. In addition, the distribution of globules and cells in relation to one another was non-random ($P < 0.001$) and suggests that globules form near cells. Using HPLC analysis of bimane-derivatized supernatants of S⁰-producing cultures (Rethmeier *et al.*, 1997), we observed two soluble thiol-containing compounds that exhibited retention times identical to those of polysulfides in a standard (Fig. 4a); these appeared to transiently accumulate during S⁰ production (Fig. S4A). Taken together, these observations suggest that cells contribute to a pool of dissolved forms of sulfur from which a set of globules nucleate in the very early stages of sulfide oxidation and continue to grow by accretion.

Attachment of some cells to S⁰ globules is required for globule degradation

During S⁰ globule degradation, fewer than 20% of cells were attached to S⁰ globules at any one time, which agreed with previous measurements of *Cba. tepidum* cultures (Hanson *et al.*, 2015). In theory, there could be globules smaller than the 0.45 µm resolution limit; however, we have never observed small S⁰ globules in cryoSEM images of S⁰-degrading cultures. Cells grew and divided during S⁰ globule degradation whether they were attached to S⁰ globules or not (Fig. 5, Video S4). S⁰ globules were degraded while in contact with cells. Unexpectedly, we also observed S⁰ globules that were degraded without any contact from cells over the duration of the degradation stage (Fig. 5).

We compared the rates of elongation for cells both attached and unattached to sulfur globules and found that there was no difference between the two populations. However, there was a weak, but statistically significant, positive relationship between cell elongation rate and globule proximity ($R^2 = 0.338$, $P = 0.047$) (Fig. 5). Doubling times were calculated from the cells that could be tracked from division as a daughter cell to a second division as a parent cell. Doubling times ranged from 2.5 to 3.2 h for both attached and unattached cells, comparable with the 2.1–2.3 h doubling times observed in batch cultures of *Cba. tepidum* (Chan *et al.*, 2008b; Morgan-Kiss *et al.*, 2009; Wahlund *et al.*, 1991).

To understand how unattached cells were able to grow, we looked for soluble sulfur intermediates in *Cba. tepidum* cultures that could feed unattached cells during the S⁰ globule degradation stage (Truper & Fischer, 1982; Van Gernerden, 1984). Within the culture supernatants, we detected an HPLC peak corresponding to polysulfide (Fig. 4b). This

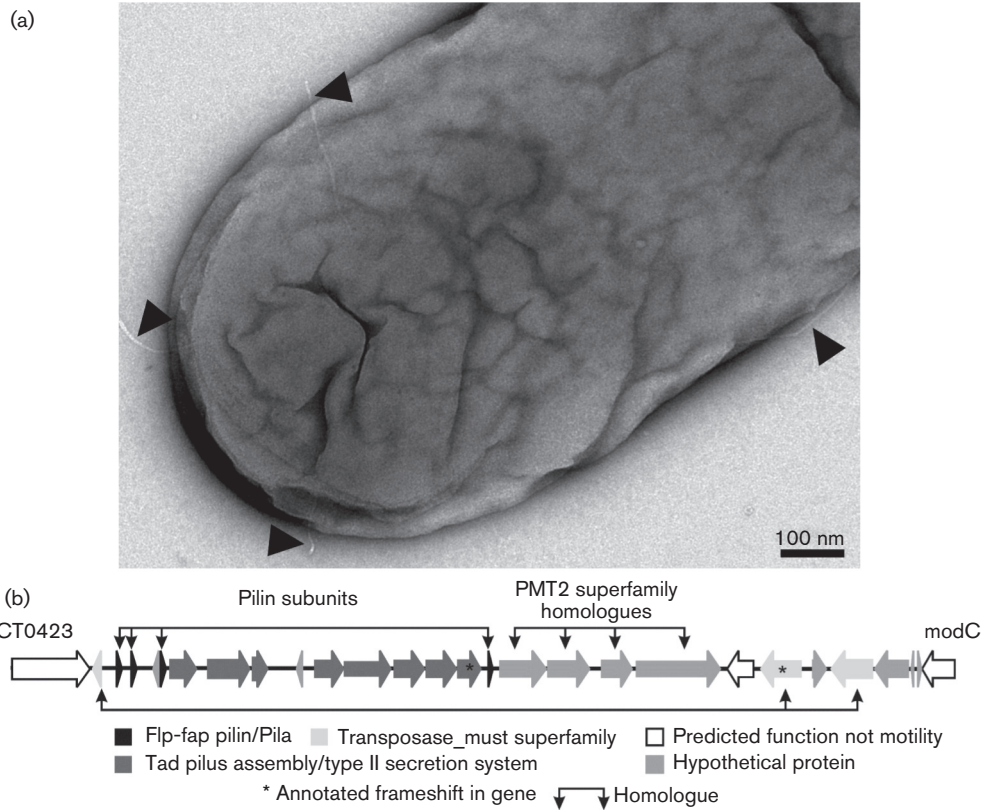


Fig. 2. (a) TEM micrograph of a *Cba. tepidum* cell with pili (black arrowheads). (b) Annotated genomic region of *Cba. tepidum* that encodes four type IV pilin subunits and assembly machinery. Shading indicates gene product function as noted in the key. Genes with annotated frame shifts are noted with asterisks and those that display significant primary amino acid sequence similarity are indicated by joined arrows.

peak increased during S⁰ degradation relative to controls (cells in sulfur-free medium and uninoculated medium with S⁰), from 0 to 30 h (Fig. S4B, C).

S⁰ globule morphology over time

S⁰ globules appeared smooth and round during the globule production stage, as observed by cryoSEM. Some S⁰ globules in contact with cells deformed slightly, suggesting

possible attraction between the cell and globule, while S⁰ globules not in contact with cells remained roughly spherical (Fig. 6a, b). This may reflect the pliability and ‘liquid’-like properties of early-stage S⁰ globules. The attachment point between cells and globules frequently occurred on the poles of the cell.

S⁰ globule morphology was observed in cultures of wild-type *Cba. tepidum* grown on purified biogenic S⁰ as the sole

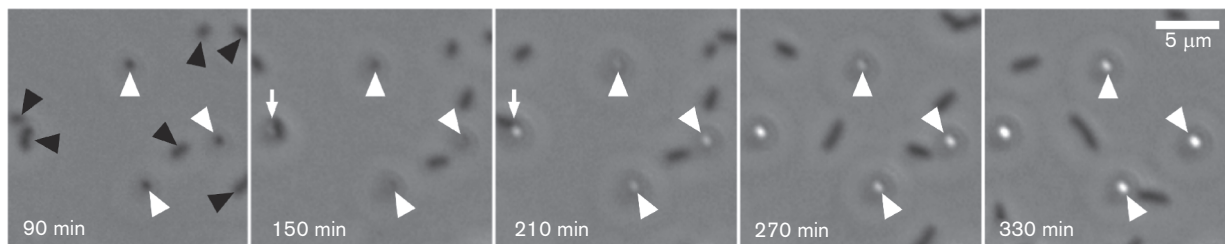


Fig. 3. Time-lapse montage of S⁰ globules (white arrowheads) growing without contact from cells (black arrowheads). A fourth S⁰ globule is in view, but receives transient cell contact (white arrows). While the montage is shown at 25 min intervals, images were taken at 1 min intervals and no contact was observed for the duration of the montage. The full movie is available as Video S1.

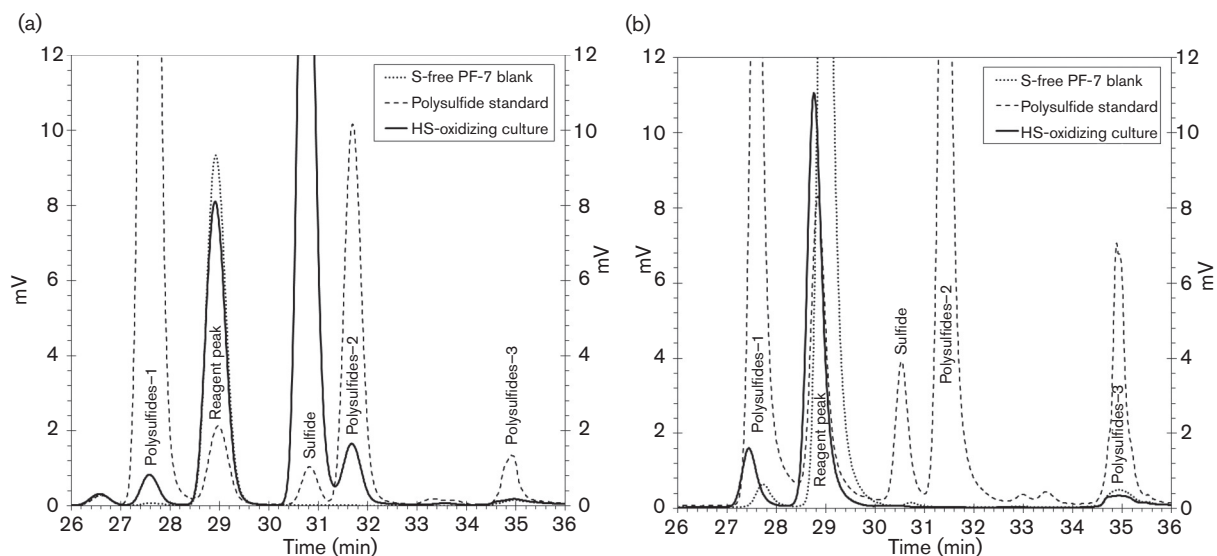


Fig. 4. Representative HPLC traces of culture supernatants from S^0 -producing *Cba. tepidum* culture grown on sulfide as the sole electron donor (a) and S^0 -degrading (b) cultures grown on biogenic S^0 as the sole electron donor. Traces for a polysulfide standard and a sulfur-free PF-7 medium blank are overlaid for comparison. The presence of polysulfide-1 and polysulfide-2 peaks are evident for the S^0 -producing culture, while the presence of only one peak with a retention time similar to polysulfide-1 is observed for the S^0 -degrading culture.

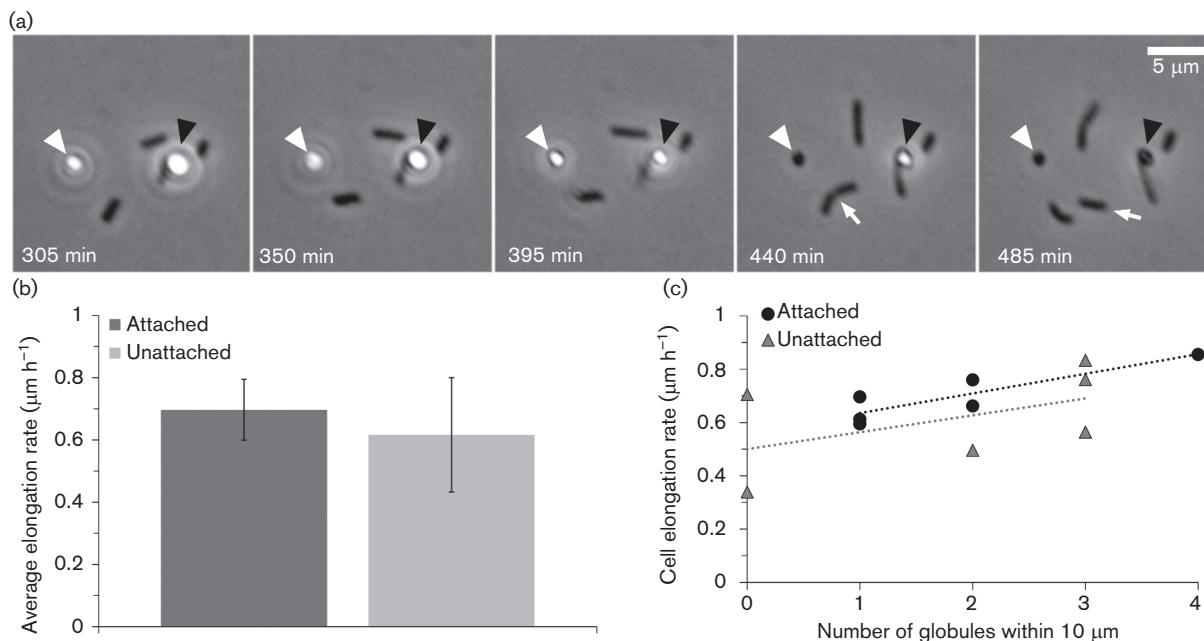


Fig. 5. (a) Time-lapse montage of S^0 globule degradation. White arrowheads show the degradation of a globule without cell contact; black arrowheads show the degradation of a globule always in contact with a cell. White arrows show an unattached cell growing, and then dividing at 470 min. These observations are observed throughout the 1 min interval time-lapse experiment. The full movie is available in Video S4. (b) Average rate of cell elongation in micrometres per hour for cells unattached and attached to S^0 globules. Cells were measured starting at 240 min of growth. Measurements were taken every 5 min until the experiment concluded at 565 min of growth; $n=6$ per condition. (c) Relationship between the number of S^0 globules within a 10 μm radius of a cell and the rate of that cell's elongation. Data points include both attached and unattached cells.

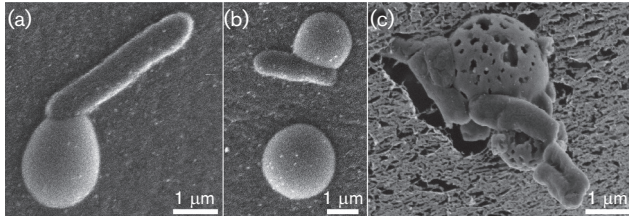


Fig. 6. CryoSEM micrographs showing S⁰ globule texture and morphology through the production and degradation stages. (a, b) Production-stage S⁰ globules and wild-type *Cba. tepidum* cells attached. (c) Partially degraded biogenic S⁰ globule with attached wild-type *Cba. tepidum* cells (panel C from Hanson *et al.*, 2015; reproduced here for comparison with production-stage globules).

electron donor [described by Hanson *et al.* (2015)]. Partially degraded S⁰ globules in these cultures were markedly different from globules observed during formation. Degradation presented as a corrosion-like morphology, with shallow and deep pits in the globule surface (Fig. 6c). This morphology highlights the fact that the apparent diameter of globules in phase contrast microscopy may not represent the true volume and morphology of S⁰ globules, particularly in the degradation stage. When cells were observed in association with degraded globules, the size of the pits was smaller than the attached surface of the cell. This suggests that such degradation is not a result of burrowing cells. The pits are often regularly distributed across the globule surface and do not appear concentrated at the location of attached cells. This suggests previous, transient contact by cells, and/or degradation of S⁰ globules by a dissolved phase.

DISCUSSION

By characterizing the spatial relationships and physical dynamics of *Cba. tepidum*-S⁰ globule interactions, we have been able to constrain the mechanisms of globule production and degradation. We found that *Cba. tepidum* deposits and dissolves S⁰ globules effectively both with contact and at a distance. The discovery of twitching motility partially explains how *Cba. tepidum* accesses extracellularly deposited S⁰ globules. The observations of S⁰ globule growth and degradation at a distance from cells can be explained by the polysulfides we observed in culture supernatants. Polysulfides have long been suggested to play a role in the production and degradation of S⁰ globules (Brune, 1995; Franz *et al.*, 2009; Truper & Fischer, 1982; van Gemerden, 1984; Visscher & van Gemerden, 1988). To our knowledge, this paper provides the first evidence for the presence of polysulfides in *Cba. tepidum* S⁰-producing and S⁰-degrading cultures. Our observations support the hypothesis that polysulfides are key intermediates of both S⁰ globule formation and degradation, which enables *Cba. tepidum* to overcome the challenges of mineral production and degradation.

An updated model of S⁰ globule production and degradation in *Cba. tepidum*

Based on our findings, we have developed an updated model of S⁰ globule production and degradation by *Cba. tepidum* (Fig. 7). In this model, *Cba. tepidum* cells oxidize sulfide to polysulfides, which diffuse into the surrounding medium. Chains of sulfur, for example polysulfides and organic polysulfanes, can cyclize (Brune, 1995; Eckert *et al.*, 2003; Garcia & Druschel, 2014; Kleinjan *et al.*, 2003; Steudel, 2003), consistent with the existence of S₈ rings in biogenic S⁰ globules (George *et al.*, 2008; Pickering *et al.*, 2001; Prange *et al.*, 2002). The pattern of rapid S⁰ globule nucleation, followed by growth but no new visible globule production, can be explained by aggregation and Ostwald particle ripening. S₈ rings can quickly aggregate into very small condensed forms of sulfur (Steudel *et al.*, 1988; Steudel, 1996, 2003), with a critical nucleus size as low as 30 nm (Chaudhuri & Paria, 2010). Attraction between these clusters causes further aggregation (Garcia & Druschel, 2014). In Ostwald ripening, growth of larger particles occurs at the expense of smaller particles, due to differences in surface energetics (Gilbert *et al.*, 2003). These processes have been shown in theoretical and experimental work to govern abiotic elemental sulfur particle growth (Garcia & Druschel, 2014).

When sulfide is exhausted, cells switch to S⁰ globule oxidation. While cells that are attached to globules can degrade them through direct contact, we have also observed that unattached cells grow and that many S⁰ globules shrink in the absence of any cell contact. These observations require that soluble compounds participate in S⁰ degradation by *Cba. tepidum*. We suggest that attached cells initiate globule degradation, producing polysulfides. Polysulfides in the medium can then carry out several functions: (1) diffuse into other cells and reach inner membrane Dsr proteins that are required for S⁰ utilization by *Cba. tepidum* (Holkenbrink *et al.*, 2011), and (2) reductively open S₈ rings in S⁰ globules, releasing more polysulfides. These functions are consistent with our observations that unattached cells grow and S⁰ globules degrade in the absence of any cell contact.

Dissolved intermediates as agents of globule production and dissolution at a distance

Our observations indicate that nearly all *Cba. tepidum* cells were growing and dividing during S⁰ globule formation and must be producing a sulfur byproduct. Our detection of polysulfides suggests that they serve as a soluble intermediate and direct mineral nucleation and S⁰ globule growth away from *Cba. tepidum* cells. This idea is supported by the production of fewer S⁰ globules than cells, suggesting that multiple cells contribute to the formation of a single globule. By directing mineral nucleation away from the cell surface, *Cba. tepidum* is able to avoid encrustation. This is in contrast to Fe oxidation and biomineralization at neutral pH, in which Fe oxides are at least initially in direct contact with cells, such as stalks (Chan *et al.*, 2011). This is probably because Fe(III) is typically insoluble at neutral pH,

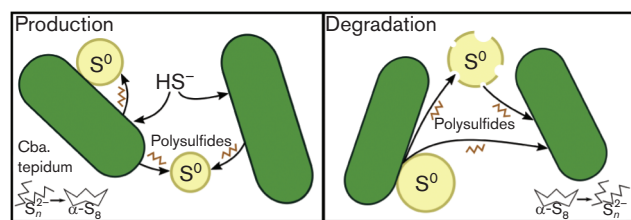


Fig. 7. Model of S^0 globule production and degradation in *Cba. tepidum*. During globule production, cells oxidize sulfide (HS^-) to a pool of intermediate, soluble polysulfide. This pool can then accrete into globules. When sulfide is exhausted, globule degradation begins. Attached cells oxidize S^0 globules and produce polysulfide intermediates. These intermediates can then (a) degrade globules at a distance from cells, and (b) feed unattached cells.

and no soluble intermediate exists to facilitate remote nucleation. In sulfur oxidation, the existence of soluble intermediates allows for remote mineral formation and growth.

Because globules are often formed at a distance from cells, it is important to consider how exactly the cells are able to find and/or utilize their sulfur when sulfide is exhausted and the S^0 globule degradation stage begins. Previous work has shown that *Cba. tepidum* will not grow on biogenic S^0 as a sole electron donor if cells and S^0 are separated by a dialysis membrane, suggesting that direct contact with S^0 globules is required for growth (Hanson *et al.*, 2015). With this requirement, there are significant challenges in finding and accessing sulfur in the degradation stage.

Our results show that these challenges can be addressed by a subpopulation oxidizing sulfur at a distance from globules. It is important to note that globule degradation and sulfur oxidation may have some overlap, but are not inherently the same process. We hypothesize that attached *Cba. tepidum* cells can dissolve S^0 through direct contact with globules and that these attached cells produce soluble intermediates, with polysulfides the most likely candidate based on our HPLC data. If flavins or other cellular metabolites could mediate interactions between *Cba. tepidum* and S^0 at a distance, then dialysis culture should have been successful, as in the case of other organisms (Fuller *et al.*, 2014; Gralnick & Newman, 2007; Lovley *et al.*, 1996; Marsili *et al.*, 2008). Because *Cba. tepidum* cannot grow when separated from S^0 , a model such as the one shown in Fig 7., involving both direct contact and remote S^0 utilization, is required.

Implications for GSB in the environment

Why would a microbe store S^0 globules extracellularly? Transient attachment suggests that cells and globules are not well attached to each other, and so this could result in other microbes pirating *Cba. tepidum* sulfur. However, if, as we suggest, attached cells produce soluble intermediates during S^0 globule degradation, presumably other SOB could

do the same and feed unattached *Cba. tepidum* cells. The S^0 globules may also be reduced by sulfur-reducing microbes to sulfide, which is the preferred electron donor for *Cba. tepidum*, thereby creating a closed syntrophic sulfur cycle. This interaction has been observed between *Chlorobium vibrioforme* strain 1930 and *Desulfuromonas acetoxidans* (Warthmann *et al.*, 1992). In either case, extracellular storage would not represent a loss, and could in fact be an advantage, as *Cba. tepidum* cells would still reap benefits from the sulfur globules they produced.

ACKNOWLEDGEMENTS

This work was supported by funds from the University of Delaware Research Foundation and NSF grant MCB-1244373 to T. E. H. and C. S. C., as well as NSF grant GRFP-0750966 to A. T. L. It also utilized infrastructure resources provided by grants from the National Science Foundation EPSCoR programme (EPS-0814251) and National Institutes of Health INBRE programme (2 P20 RR016472-09) from the National Center for Research Resources. We thank Shannon Modla for help with TEM sample preparation and imaging, Mike Moore and Jeff Caplan for helpful discussions during development of the methods of the time-lapse microscopy setup, and Jeff Caplan for assistance with time-lapse image analysis. We also thank Kara Hoppes, Erin Field, Shingo Kato and Sean McAllister for helpful discussion and comments on the manuscript.

REFERENCES

- Beliaev, A. S. & Saffarini, D. A. (1998). *Shewanella putrefaciens mtrB* encodes an outer membrane protein required for Fe(III) and Mn(IV) reduction. *J Bacteriol* **180**, 6292–6297.
- Berry, J. L. & Pelicic, V. (2015). Exceptionally widespread nanomachines composed of type IV pilins: the prokaryotic Swiss Army knives. *FEMS Microbiol Rev* **39**, fuu001.
- Brocher, J. (2015). The BioVoxel image processing and analysis toolbox. In European BioImage Analysis Symposium. Paris, France.
- Brune, D. C. (1995). Isolation and characterization of sulfur globule proteins from *Chromatium vinosum* and *Thiocapsa roseopersicina*. *Arch Microbiol* **163**, 391–399.
- Bryant, D. A. & Frigaard, N. U. (2006). Prokaryotic photosynthesis and phototrophy illuminated. *Trends Microbiol* **14**, 488–496.
- Burrows, L. L. (2012). *Pseudomonas aeruginosa* twitching motility: type IV pili in action. *Annu Rev Microbiol* **66**, 493–520.
- Chan, L.-K., Morgan-Kiss, R. & Hanson, T. E. (2008a). Genetic and proteomic studies of sulfur oxidation in *Chlorobium tepidum* (syn. *Chlorobaculum tepidum*). In *Sulfur Metabolism in Phototrophic Organisms*, pp. 357–373. Springer.
- Chan, L.-K., Morgan-Kiss, R. & Hanson, T. E. (2008b). Sulfur oxidation in *Chlorobium tepidum* (syn. *Chlorobaculum tepidum*): genetic and proteomic analyses. In *Microbial Sulfur Metabolism*, pp. 117–126. Edited by C. Dahl & C. G. Friedrich. Berlin/Heidelberg: Springer.
- Chan, L.-K., Weber, T. S., Morgan-Kiss, R. M. & Hanson, T. E. (2008c). A genomic region required for phototrophic thiosulfate oxidation in the green sulfur bacterium *Chlorobium tepidum* (syn. *Chlorobaculum tepidum*). *Microbiology* **154**, 818–829.
- Chan, C. S., Fakra, S. C., Emerson, D., Fleming, E. J. & Edwards, K. J. (2011). Lithotrophic iron-oxidizing bacteria produce organic stalks to control mineral growth: implications for biosignature formation. *ISME J* **5**, 717–727.

- Chaudhuri, R. G. & Paria, S. (2010).** Synthesis of sulfur nanoparticles in aqueous surfactant solutions. *J Colloid Interface Sci* **343**, 439–446.
- Dahl, C. & Prange, A. (2006).** Bacterial sulfur globules: occurrence, structure and metabolism. In *Inclusions in Prokaryotes*, pp. 21–51. Edited by J. M. Shively. Berlin/Heidelberg: Springer.
- Donà, C. (2011).** Mobilization of sulfur by green sulfur bacteria: physiological and molecular studies on *Chlorobaculum parvum* DSM 263. *Chemie der Universität Bremen*, Bremen.
- Eckert, B., Okazaki, R., Steudel, R., Takeda, N., Tokitoh, N. & Wong, M. (2003).** Elemental sulfur and sulfur-rich compounds II. *Top Curr Chem* **231**, 32–98.
- Franz, B., Lichtenberg, H., Hormes, J., Modrow, H., Dahl, C. & Prange, A. (2007).** Utilization of solid 'elemental' sulfur by the phototrophic purple sulfur bacterium *Allochromatium vinosum*: a sulfur K-edge X-ray absorption spectroscopy study. *Microbiology* **153**, 1268–1274.
- Franz, B., Gehrke, T., Lichtenberg, H., Hormes, J., Dahl, C. & Prange, A. (2009).** Unexpected extracellular and intracellular sulfur species during growth of *Allochromatium vinosum* with reduced sulfur compounds. *Microbiology* **155**, 2766–2774.
- Friedrich, C. G., Rother, D., Bardischewsky, F., Quentmeier, A. & Fischer, J. (2001).** Oxidation of reduced inorganic sulfur compounds by bacteria: emergence of a common mechanism? *Appl Environ Microbiol* **67**, 2873–2882.
- Frigaard, N.-U. & Dahl, C. (2008).** Sulfur metabolism in phototrophic sulfur bacteria. *Adv Microb Physiol* **54**, 103–200.
- Fuller, S. J., McMillan, D. G., Renz, M. B., Schmidt, M., Burke, I. T. & Stewart, D. I. (2014).** Extracellular electron transport-mediated Fe(III) reduction by a community of alkaliphilic bacteria that use flavins as electron shuttles. *Appl Environ Microbiol* **80**, 128–137.
- Garcia, A. A. & Druschel, G. K. (2014).** Elemental sulfur coarsening kinetics. *Geochem Trans* **15**.
- George, G. N., Gnida, M., Bazylinski, D. A., Prince, R. C. & Pickering, I. J. (2008).** X-ray absorption spectroscopy as a probe of microbial sulfur biochemistry: the nature of bacterial sulfur globules revisited. *J Bacteriol* **190**, 6376–6383.
- Gilbert, B., Zhang, H., Huang, F., Finnegan, M. P., Waychunas, G. A. & Banfield, J. F. (2003).** Special phase transformation and crystal growth pathways observed in nanoparticles. *Geochem Trans* **4**, 20–27.
- Gralnick, J. A. & Newman, D. K. (2007).** Extracellular respiration. *Mol Microbiol* **65**, 1–11.
- Gregersen, L. H., Bryant, D. A. & Frigaard, N. U. (2011).** Mechanisms and evolution of oxidative sulfur metabolism in green sulfur bacteria. *Front Microbiol* **2**.
- Hanson, T. E., Bonsu, E., Tuerk, A., Marnocha, C. L., Powell, D. H. & Chan, C. S. (2015).** *Chlorobaculum tepidum* growth on biogenic S⁰ as the sole photosynthetic electron donor. *Environ Microbiol*.
- Hegler, F., Schmidt, C., Schwarz, H. & Kappler, A. (2010).** Does a low-pH microenvironment around phototrophic Fe(II)-oxidizing bacteria prevent cell encrustation by Fe(III) minerals? *FEMS Microbiol Ecol* **74**, 592–600.
- Holkenbrink, C., Barbas, S. O., Mellerup, A., Otaki, H. & Frigaard, N. U. (2011).** Sulfur globule oxidation in green sulfur bacteria is dependent on the dissimilatory sulfite reductase system. *Microbiology* **157**, 1229–1239.
- Kachlany, S. C., Planet, P. J., Desalle, R., Fine, D. H., Figurski, D. H. & Kaplan, J. B. (2001).** flp-1, the first representative of a new pilin gene subfamily, is required for non-specific adherence of *Actinobacillus actinomyces-comitans*. *Mol Microbiol* **40**, 542–554.
- Kleinjan, W. E., de Keizer, A., & Janssen, A. J. (2003).** Biologically produced sulfur. In *Elemental Sulfur and Sulfur-Rich Compounds I*, pp. 167–188. Edited by R. Steudel. Berlin/Heidelberg: Springer Verlag.
- Lloyd, J. R. (2003).** Microbial reduction of metals and radionuclides. *FEMS Microbiol Rev* **27**, 411–425.
- Lloyd, J. R., Blunt-Harris, E. L. & Lovley, D. R. (1999).** The periplasmic 9.6-kilodalton c-type cytochrome of *Geobacter sulfurreducens* is not an electron shuttle to Fe(III). *J Bacteriol* **181**, 7647–7649.
- Lovley, D. R., Coates, J. D., Blunt-Harris, E. L., Phillips, E. J. P. & Woodward, J. C. (1996).** Humic substances as electron acceptors for microbial respiration. *Nature* **382**, 445–448.
- Maier, B. & Wong, G. C. (2015).** How bacteria use type IV pili machinery on surfaces. *Trends Microbiol* **23**, 775–788.
- Mangold, S., Valdés, J., Holmes, D. S. & Dopson, M. (2011).** Sulfur metabolism in the extreme acidophile *Acidithiobacillus caldus*. *Front Microbiol* **2**.
- Marsili, E., Baron, D. B., Shikhare, I. D., Coursolle, D., Gralnick, J. A. & Bond, D. R. (2008).** *Shewanella* secretes flavins that mediate extracellular electron transfer. *Proc Natl Acad Sci U S A* **105**, 3968–3973.
- Morgan-Kiss, R. M., Chan, L. K., Modla, S., Weber, T. S., Warner, M., Czymmek, K. J. & Hanson, T. E. (2009).** *Chlorobaculum tepidum* regulates chlorosome structure and function in response to temperature and electron donor availability. *Photosynth Res* **99**, 11–21.
- Myers, C. R. & Myers, J. M. (1992).** Localization of cytochromes to the outer membrane of anaerobically grown *Shewanella putrefaciens* MR-1. *J Bacteriol* **174**, 3429–3438.
- Overmann, J. & Garcia-Pichel, F. (2013).** The phototrophic way of life. In *The Prokaryotes*, pp. 203–257. Edited by E. Rosenberg, E. F. DeLong, S. Lory, E. Stackebrandt & F. Thompson. Berlin/Heidelberg: Springer.
- Pibernat, I. V. & Abella, C. A. (1996).** Sulfide pulsing as the controlling factor of spinae production in *Chlorobium limicola* strain UdG 6038. *Arch Microbiol* **165**, 272–278.
- Pickering, I. J., George, G. N., Yu, E. Y., Brune, D. C., Tuschak, C., Overmann, J., Beatty, J. T. & Prince, R. C. (2001).** Analysis of sulfur biochemistry of sulfur bacteria using X-ray absorption spectroscopy. *Biochemistry* **40**, 8138–8145.
- Prange, A., Chauvistré, R., Modrow, H., Hormes, J., Trüper, H. G. & Dahl, C. (2002).** Quantitative speciation of sulfur in bacterial sulfur globules: X-ray absorption spectroscopy reveals at least three different species of sulfur. *Microbiology* **148**, 267–276.
- Rethmeier, J., Rabenstein, A., Langer, M. & Fischer, U. (1997).** Detection of traces of oxidized and reduced sulfur compounds in small samples by combination of different high-performance liquid chromatography methods. *J Chromatogr A* **760**, 295–302.
- Saini, G. & Chan, C. S. (2013).** Near-neutral surface charge and hydrophilicity prevent mineral encrustation of Fe-oxidizing micro-organisms. *Geobiology* **11**, 191–200.
- Schindelin, J., Arganda-Carreras, I., Frise, E., Kaynig, V., Longair, M., Pietzsch, T., Preibisch, S., Rueden, C., Saalfeld, S. & other authors (2012).** Fiji: an open-source platform for biological-image analysis. *Nat Methods* **9**, 676–682.
- Shi, L., Richardson, D. J., Wang, Z., Kerisit, S. N., Rosso, K. M., Zachara, J. M. & Fredrickson, J. K. (2009).** The roles of outer membrane cytochromes of *Shewanella* and *Geobacter* in extracellular electron transfer. *Environ Microbiol Rep* **1**, 220–227.
- Steudel, R. (1996).** Mechanism for the formation of elemental sulfur from aqueous sulfide in chemical and microbiological desulfurization processes. *Ind Eng Chem Res* **35**, 1417–1423.
- Steudel, R. (2003).** Aqueous sulfur sols. In *Elemental Sulfur and Sulfur-Rich Compounds I*, pp. 153–166. Edited by R. Steudel. Berlin/Heidelberg: Springer Verlag.
- Steudel, R., Göbel, T. & Holdt, G. (1988).** The molecular composition of hydrophilic sulfur sols prepared by acid decomposition of thiosulfate. *Z Naturforsch C* **43**, 203–218.

Then, J. & Trüper, H. G. (1984). Utilization of sulfide and elemental sulfur by *Ectothiorhodospira halochloris*. *Arch Microbiol* **139**, 295–298.

Truper, H. G. & Fischer, U. (1982). Anaerobic oxidation of sulphur compounds as electron donors for bacterial photosynthesis. *Philos Trans R Soc Lond B Biol Sci* **298**, 529–542.

Trüper, H. G. & Genovese, S. (1968). Characterization of photosynthetic sulfur bacteria causing red water in Lake Faro (Messina, Sicily). *Limnol Oceanogr* **13**, 225–232.

Van Gernerden, H. (1984). The sulfide affinity of phototrophic bacteria in relation to the location of elemental sulfur. *Arch Microbiol* **139**, 289–294.

van Gernerden, H. (1986). Production of elemental sulfur by green and purple sulfur bacteria. *Arch Microbiol* **146**, 52–56.

Visscher, P. T. & van Gernerden, H. (1988). Growth of *Chlorobium limicola* f. *thiosulfatophilum* on polysulfides. In *Green Photosynthetic Bacteria*, pp. 287–294. Edited by J. M. Olson, J. G. Ormerod, J. Amesz, E. Stackebrandt, & H. G. Trüper. Springer.

Wahlund, T. M., Woese, C. R., Castenholz, R. W. & Madigan, M. T. (1991). A thermophilic green sulfur bacterium from New Zealand hot springs, *Chlorobium tepidum* sp. nov. *Arch Microbiol* **156**, 81–90.

Warthmann, R., Cypionka, H. & Pfennig, N. (1992). Photoproduction of H₂ from acetate by syntrophic cocultures of green sulfur bacteria and sulfur-reducing bacteria. *Arch Microbiol* **157**, 343–348.

Edited by: C. Dahl